The EMBO Journal (2011) 30, 2350–2363 | © 2011 European Molecular Biology Organization | All Rights Reserved 0261-4189/11
www.embojournal.org

THE EMBO JOURNAL

AT1R–CB_1R heteromerization reveals a new mechanism for the pathogenic properties of angiotensin II

Raphael Rozenfeld[1,3], Achla Gupta[1], Khatuna Gagnidze[1], Maribel P Lim[1], Ivone Gomes[1], Dinah Lee-Ramos[1], Natalia Nieto[2,3] and Lakshmi A Devi[1,*]

[1]Department of Pharmacology and Systems Therapeutics, New York Mount Sinai School of Medicine, New York, NY, USA, [2]Department of Medicine, New York Mount Sinai School of Medicine, New York, NY, USA and [3]Alcoholic Liver Disease Research Center, New York Mount Sinai School of Medicine, New York, NY, USA

The mechanism of G protein-coupled receptor (GPCR) signal integration is controversial. While GPCR assembly into hetero-oligomers facilitates signal integration of different receptor types, cross-talk between Gαi- and Gαq-coupled receptors is often thought to be oligomerization independent. In this study, we examined the mechanism of signal integration between the Gαi-coupled type I cannabinoid receptor (CB_1R) and the Gαq-coupled AT1R. We find that these two receptors functionally interact, resulting in the potentiation of AT1R signalling and coupling of AT1R to multiple G proteins. Importantly, using several methods, that is, co-immunoprecipitation and resonance energy transfer assays, as well as receptor- and heteromer-selective antibodies, we show that AT1R and CB_1R form receptor heteromers. We examined the physiological relevance of this interaction in hepatic stellate cells from ethanol-administered rats in which CB_1R is upregulated. We found a significant upregulation of AT1R–CB_1R heteromers and enhancement of angiotensin II-mediated signalling, as compared with cells from control animals. Moreover, blocking CB_1R activity prevented angiotensin II-mediated mitogenic signalling and profibrogenic gene expression. These results provide a molecular basis for the pivotal role of heteromer-dependent signal integration in pathology.

The EMBO Journal (2011) **30,** 2350–2363. doi:10.1038/emboj.2011.139; Published online 3 May 2011
Subject Categories: signal transduction; molecular biology of disease
Keywords: endocannabinoid; GPCR heteromerization; hepatic stellate cells; liver fibrosis; signal integration

*Corresponding author. Department of Pharmacology and Systems Therapeutics, Mount Sinai School of Medicine, 19-84 Annenberg Building, One Gustave L. Levy Place, New York, NY 10029, USA. Tel.: +1 212 241 8345; Fax: +1 212 996 7214; E-mail: lakshmi.devi@mssm.edu

Received: 19 January 2011; accepted: 5 April 2011; published online: 3 May 2011

Introduction

The angiotensin II (Ang II) type 1 receptor (AT1R) is a G protein-coupled receptor (GPCR) that transduces the main physiological actions of the renin-angiotensin system in target cells. The major signalling events following agonist binding to this receptor are activation of phospholipase C via a Gαq protein, mobilization of calcium from intracellular stores, and activation of other signalling pathways such as the MAP kinase pathway that participates in the hypertrophic actions of Ang II (Clauser *et al*, 1996). AT1R is primarily involved in the control of blood pressure as demonstrated in numerous animal models (Ito *et al*, 1995; Sugaya *et al*, 1995; Le *et al*, 2003). Using functional complementation experiments, AT1R was among the first class A GPCR to be proposed to function as a dimer (Monnot *et al*, 1996), and formation of AT1R heteromers was later found to be involved in pathology (Barki-Harrington, 2004). For instance, the contribution of AT1R to specific forms of hypertension has been shown to be regulated by interactions with B2 bradykinin receptor (AbdAlla *et al*, 2001), and recently, physical interactions with the apelin receptor was proposed to regulate the atherosclerotic effect of Ang II (Chun *et al*, 2008), suggesting that heteromerization of AT1R with other GPCRs contributes to the pathophysiological effects of Ang II. In addition to its role in blood pressure regulation, AT1R hypertrophic properties contribute to the development of fibrosis in a number of organs. However, the molecular or cellular events that cause AT1R to become profibrogenic remain elusive.

Type I cannabinoid receptor (CB_1R) is widely expressed in the brain and essentially absent in peripheral tissues under normal conditions. The development of an antibody specifically recognizing the dimeric CB_1R demonstrated that this receptor exists as homodimers (Wager-Miller *et al*, 2002). In addition, CB_1R has been shown to form heteromers with a number of other GPCRs, leading to an alteration in receptor coupling as in the case of CB_1R–D2 dopamine receptor (Kearn *et al*, 2005), trafficking, as in the case of CB_1R–orexin-1 receptor (Ellis *et al*, 2006), and signalling, as in the case of CB_1R–A2aR (Carriba *et al*, 2007).

CB_1R is upregulated in some peripheral tissues during chronic diseases, such as liver fibrosis. CB_1R exhibits marginal expression in the normal liver but a robust expression in fibrotic liver, predominantly in activated hepatic stellate cells (HSCs) (Teixeira-Clerc *et al*, 2006); these cells are primarily responsible for the fibrogenic response in the liver (Friedman, 2008). HSCs also express AT1R (Pereira *et al*, 2009), and both AT1R and CB_1R antagonists exhibit anti-fibrotic properties (Teixeira-Clerc *et al*, 2006; Schuppan and Afdhal, 2008).

Here, we propose that enhanced CB_1R expression in activated HSCs could affect AT1R properties and contribute to the profibrogenic effect of Ang II. Given the implication of heteromerization in the pathophysiological function of both CB_1R and AT1R, it was of interest to determine whether such

 ©2011 European Molecular Biology Organization

a AT1R–CB$_1$R heteromer exists and could be selectively targeted pharmacologically, or if cross-talk between AT1R and CB$_1$R could result from heteromerization-independent functional interactions, as previously reported for other Gαq- and Gαi-coupled receptor pairs (Rives *et al*, 2009).

We first probed the interaction between AT1R and CB$_1$R in recombinant systems using biophysical and biochemical methods and found that the two receptors associate. This association leads to changes in coupling and enhanced signalling by AT1R that could be blocked by heteromer-selective antibodies. We also found that the AT1R-mediated signalling is controlled by CB$_1$R. For example, basal endocannabinoid tone enhances Ang II-mediated signalling and CB$_1$R antagonists block AT1R-mediated signalling. We then examined the consequences of AT1R–CB$_1$R interaction on Ang II-mediated profibrogenic responses in activated HSCs. We show that AT1R interacts with CB$_1$R to form heteromers in these cells, and this facilitates the profibrogenic effect of Ang II. These results provide evidence for the contribution of heteromer-directed signal specificity in pathology.

Results

Ang II-mediated ERK phosphorylation is altered in the presence of CB$_1$R

We first examined the effect of CB$_1$R coexpression on AT1R signalling. We took advantage of Neuro2A cells, a neuroblastoma cell line that contains endogenous CB$_1$R to examine

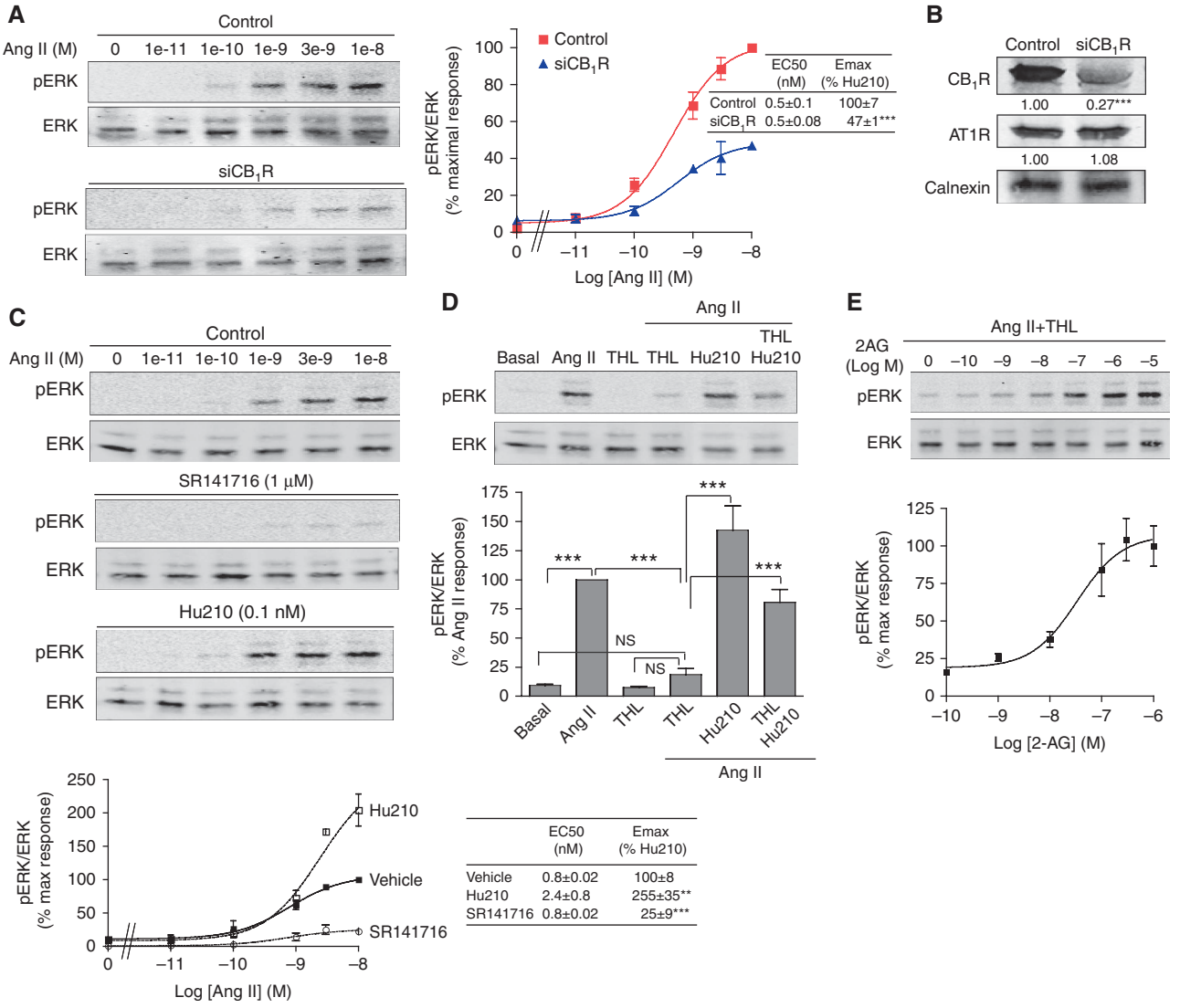

Figure 1 CB$_1$R modulates AT1R signalling. (**A**) Neuro2A-AT1R cells transfected or not with a siRNA to CB$_1$R were stimulated with increasing concentrations of Ang II for 3 min. Data represent mean ± s.e.m. ($n = 3$–5). ***$P < 0.001$. (**B**) Representative western blot analysis of Neuro2A-AT1R cells transfected with control or CB$_1$R-targeting siRNA and probed for the levels of CB$_1$R (~70% decrease with CB$_1$R siRNA), AT1R (no change) and calnexin as a loading control. Mean ± s.e.m. densitometry from three independent transfections are indicated below the western blot. ***$P < 0.001$. (**C**) Neuro2A-AT1R cells starved for 4 h, were stimulated with increasing concentrations of Ang II for 3 min, in the presence of the CB$_1$R antagonist (SR141716; 1 μM) or in the presence of a non-signalling dose of the CB$_1$R agonist (Hu210; 0.1 nM). Data represent mean ± s.e.m. ($n = 3$–5). **$P < 0.01$; ***$P < 0.001$. (**D**) Phospho-ERK levels after Ang II stimulation were examined in Neuro2A-AT1R cells, after treatment with the diacylglycerol lipase inhibitor THL (1 μM; 2 h pretreatment) alone or together with Hu210 (0.1 nM); or, (**E**) with increasing concentrations of 2-AG. Data are expressed as the mean ± s.e.m. ($n = 3$–4). **$P < 0.01$; ***$P < 0.001$; NS, non-significant. Cell lysates were subjected to western blotting analysis using antibodies to pERK and ERK (1:1000). Imaging and quantification was carried out using the Odyssey Imaging system (Li-Core Biosciences).

©2011 European Molecular Biology Organization

functional interactions of CB_1R with AT1R. For this, we generated stable cell lines expressing an N-terminally Flag-tagged AT1R (Neuro2A-AT1R), and explored the modulation of AT1R function by CB_1R. Stimulation with Ang II led to a rapid, robust, and dose-dependent increase in pERK levels (Figure 1A; Supplementary Figure S1A). This was blocked by pretreatment with the specific AT1R antagonist Losartan, and was dependent on AT1R since wild-type (non-transfected) Neuro2A cells did not respond to Ang II (Supplementary Figure S1A). We examined if the presence of CB_1R contributed to the response of AT1R to Ang II stimulation, by directly altering CB_1R expression. RNAi-mediated CB_1R downregulation (see Figure 1B) led to a dramatic decrease (by $\sim$50%) in Ang II-mediated signalling (Figure 1A; Supplementary Figure S1A). Dose response experiments indicated that CB_1R affects AT1R signalling by increasing the efficacy of Ang II (Figure 1A).

CB_1R activation determines Ang II efficacy

Next, we examined the extent of involvement of CB_1R activity in Ang II-mediated signalling using CB_1R-specific ligands. The CB_1R selective antagonist SR141716 (rimonabant) blocked by >70% Ang II response (Figure 1C) while the CB_1R agonist Hu210 potentiated this response (Figure 1C). Since CB_1R antagonist blocked AT1R signalling, we hypothesized that in the absence of exogenous CB_1R ligand, CB_1R-mediated increase in Ang II efficacy could be the result of activation of CB_1R by endocannabinoids. We tested this possibility by inhibiting the production of the endocannabinoid 2-arachidonoyl glycerol (2-AG). Blocking the enzyme, diacylglycerol lipase (DAGL), responsible for 2-AG production, with the DAGL inhibitor THL, led to a complete blockade of Ang II response (Figure 1D). We also examined if the addition of exogenous CB_1R agonists (Hu210 or 2-AG) could reverse the effect of THL treatment. In the presence of THL, addition of Hu210 or 2-AG was able to restore Ang II-mediated signalling (Figure 1E). The effect of cannabinoid ligands on Ang II-mediated ERK phosphorylation was not observed upon RNAi-mediated downregulation of CB_1R (Supplementary Figure S1B). The potentiating effect of CB_1R activity on Ang II-mediated signalling was not restricted to ERK signalling, since other signalling events such as Ang II-induced p38 and JNK phosphorylation were also attenuated by downregulating CB_1R (Supplementary Figure S2A). Blockade of Ang II-mediated ERK phosphorylation by SR141716 or by THL could also be seen in HEK293 cells coexpressing AT1R and CB_1R, but not in cells expressing AT1R alone (Supplementary Figure S2B). Together, these data indicate that AT1R signalling is controlled by CB_1R activity. In the absence of exogenous cannabinoid ligands, endocannabinoid-mediated basal CB_1R activation is sufficient to allow and potentiate AT1R signalling.

AT1R physically interacts with CB_1R

Using a variety of approaches, we examined if the functional interaction between CB_1R and AT1R was the consequence of physical interaction (heteromerization) between these two receptors. First, we carried out co-immunoprecipitation experiments and detected interaction between CB_1R and AT1R only in cells coexpressing the two receptors (Figure 2A). This interaction was also supported by colocalization of Flag–AT1R with CB_1R in Neuro2A-AT1R cells (Figure 2B). Since individually expressed AT1R is at the plasma membrane and CB_1R is in intracellular compartments (Pignatari *et al*, 2006; Rozenfeld and Devi, 2008), we examined changes in CB_1R and AT1R localization upon coexpression of the receptors in HEK293 cells (Supplementary Figure S2C). We find that when coexpressed with AT1R, CB_1R was found primarily at the plasma membrane colocalized with AT1R (Supplementary Figure S2D), supporting an association between the two receptors since such a change in receptor localization has been previously reported to be due to receptor heteromerization (Ellis *et al*, 2006).

We then used bioluminescence resonance energy transfer (BRET) technology that allows the detection of energy trans-

Figure 2 Interaction between AT1R and CB_1R. (**A**) Association of AT1R and CB_1R in Neuro2A-AT1R. Lysates from Neuro2A and Neuro2A-AT1R were subjected to immunoprecipitation using a protein A agarose-coupled anti-CB_1R antibody (1 μg), and to western blotting analysis with an anti-AT1R antibody (1:200). AT1R is detected in the CB_1R immunoprecipitate from Neuro2A-AT1R. (**B**) Immunofluorescence and confocal microscopy analysis of Neuro2A cells expressing endogenous CB_1R and of Neuro2A cells stably expressing Flag–AT1R. Cells grown on coverslips were fixed with 4% PFA, permeabilized in 0.1% Triton X-100, and stained with primary rabbit polyclonal anti-CB_1R (1:500) and mouse monoclonal M2 anti-Flag (1:1000) antibodies. After fluorescent secondary antibody staining, the coverslips were mounted with mowiol. Slides were examined with a Leica SP5 confocal microscope. (**C**) Detection of AT1R–CB_1R heteromers by BRET in living HEK293 cells. BRET experiments were carried out using C-terminally Renilla luciferase-tagged CB_1R, and eGFP-tagged AT1R ($\sim$400–500 fmol receptor/mg protein). BRET ratio was measured in cells expressing the indicated constructs. To assess the specificity of interaction, BRET ratios were measured in cells coexpressing increasing concentrations of untagged AT1R, in cells coexpressing untagged endothelin converting enzyme-2, or in cells coexpressing MOR–Luc with AT1R–eGFP. In addition, BRET saturation curve was generated (insert). HEK-293 cells were co-transfected with a constant DNA concentration of CB_1R–Rluc and increasing DNA concentrations of AT1R–eGFP. Curves were fitted using a non-linear regression equation assuming a single binding site (GraphPad Prism). Results are mean values ± s.e.m. ($n=3$ experiments). ***$P<0.001$; NS, non-significant, versus CB_1R–Luc/AT1R–eGFP. (**D**) Detection of AT1R–CB_1R heteromers with heteromer-selective monoclonal antibodies. Receptor abundance was determined in Neuro2A, Neuro2A-AT1R, and Neuro2A-AT1R cells where CB_1R was downregulated by RNAi (Neuro2A-AT1R siCB_1R) with a monoclonal antibody to AT1R–CB_1R, or polyclonal antibodies to AT1R or CB_1R by ELISA. Results are mean values ± s.e.m. ($n=3$ experiments). ***$P<0.001$; NS, non-significant, versus Neuro2A-AT1R. (**E**) Inhibition of AT1R–CB_1R signalling by the AT1R–CB_1R heteromer antibody. Neuro2A-AT1R and Neuro2A-AT1R cells where CB_1R was downregulated by RNAi (Neuro2A-AT1R/siCB_1R) were incubated with increasing concentrations of the monoclonal anti-AT1R–CB_1R antibody (hydridoma supernatant, +, 1:20 v/v; ++, 1:10 v/v; +++, 1:5 v/v; ++++, 2:5 v/v) for 30 min, and then were stimulated with 10 nM Ang II for 3 min. Cell lysates and media were subjected to western blotting analysis using antibodies to pERK and ERK (1:1000) (lysate) and anti-mouse IgG (media). Imaging and quantification were carried out using the Odyssey Imaging system (Li-Core Biosciences). Results are mean values ± s.e.m. ($n=4$ experiments). ***$P<0.001$; NS, non-significant, versus the corresponding Ang II treatment. (**F**) [^{35}S]GTPγS-binding assay. Membranes from Neuro2A-AT1R cells were treated with increasing concentrations of the AT1R agonist Ang II, in the absence or presence of the CB_1R antagonist PF514273 (1 μM). [^{35}S]GTPγS binding was measured as described in 'Materials and methods'. Results are mean values ± s.e.m. ($n=3$ experiments). ***$P<0.001$. (**G**) Reciprocal regulation of CB_1R signalling by AT1R. Neuro2A or Neuro2A-AT1R cells were incubated in the presence of increasing concentrations of Hu210 for 5 min, in the absence or presence or 0.01 nM Ang II. Data represent mean ± s.e.m. ($n=3$). ***$P<0.001$.

 ©2011 European Molecular Biology Organization

fer between one receptor bearing the BRET donor (Renilla luciferase) and the second receptor bearing the acceptor (green fluorescent protein) when the two receptors are in close proximity (<50 Å) (Angers *et al*, 2000). Under these conditions, we observed a highly significant BRET signal in cells coexpressing tagged AT1R and CB$_1$R (Figure 2C). No

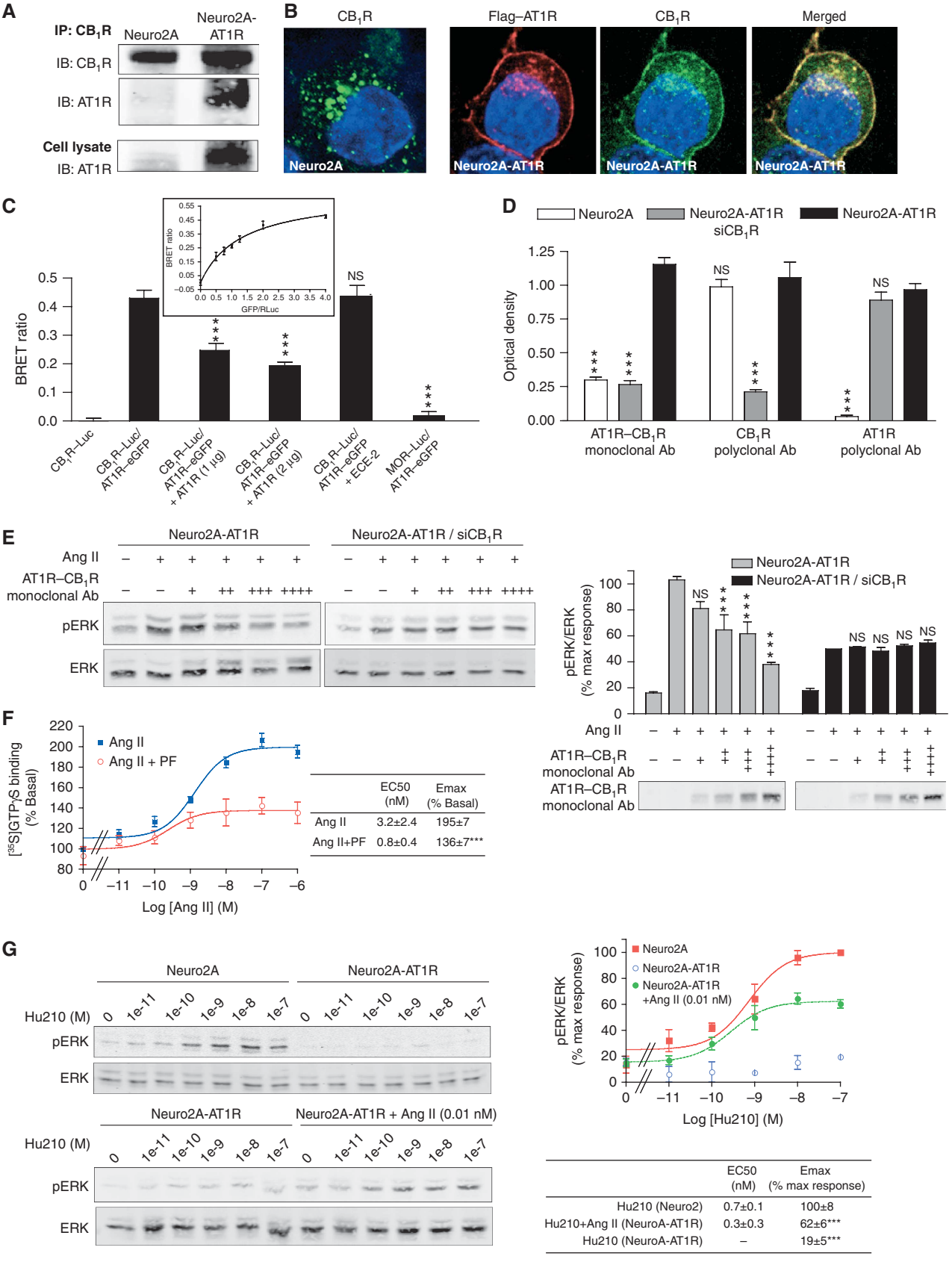

©2011 European Molecular Biology Organization

significant BRET signal was observed in cells coexpressing mu opioid receptor (MOR)–Luc and AT1R–eGFP. The BRET signal between AT1R and CB_1R was decreased upon coexpression of untagged AT1R, but not another membrane protein, endothelin converting enzyme-2, indicating competition between the tagged and untagged AT1R for interaction with CB_1R and the specificity of AT1R–CB_1R interaction.

Finally, we detected AT1R–CB_1R heteromers using heteromer-specific antibodies. For this, we developed monoclonal antibodies specifically directed against the AT1R–CB_1R heteromer using a strategy employed for the generation of monoclonal antibodies against the MOR–delta opioid receptor (DOR) heteromer (Gupta *et al*, 2010); these antibodies are useful to monitor the changes in heteromer abundance in different pathophysiological paradigms. For the subtractive immunization strategy, mice were first made tolerant to non-preferred epitopes on membrane proteins by the simultaneous administration of Neuro2A cell membranes and cyclophosphamide, which causes the death of antibody-generating activated B cells (Salata *et al*, 1992; Sleister and Rao, 2001, 2002). Once a low titre to Neuro2A cell membrane proteins was achieved, mice were immunized with membranes from Neuro2A cells coexpressing AT1R–CB_1R (desired epitope). The spleens of mice with high antibody titres were used to generate monoclonal antibodies. The supernatants from the resultant hybridoma clones were screened with Neuro2A cell membranes alone, membranes from HEK293 cells expressing only AT1R, and membranes from Neuro2A cells coexpressing both AT1R and CB_1R. This led to the identification of a number of antibody-secreting clones that gave a high signal with membranes from cells coexpressing AT1R and CB_1R, but not with membranes from cells expressing only AT1R or CB_1R (Supplementary Figure S3A), nor with cells coexpressing CB_1R with CB_2R, DOR, MOR, or KOR, or cells expressing DOR with KOR or MOR (Supplementary Figure S3B). To further characterize the specificity of the antibody, we used cells expressing different ratios of CB_1R and AT1R and find that there is maximal recognition by the heteromer antibody only when CB_1R and AT1R are expressed at similar levels (but not when the relative levels of one or the other receptor was significantly altered) (Supplementary Figure S3C). Finally, we examined the specificity of these antibodies, by their ability to detect the AT1R–CB_1R epitope in Neuro2A, Neuro2A-AT1R, and Neuro2A-AT1R in which CB_1R expression was downregulated by RNAi. We find that the antibodies recognized the specific AT1R–CB_1R epitope only in Neuro2A-AT1R, but not in cells where one of the receptors is absent or downregulated (Figure 2D). Taken together, these results indicate that the antibodies exhibit heteromer specificity and can be used to study AT1R–CB_1R heteromer properties. We then used the heteromer-specific antibody to block AT1R–CB_1R heteromer-mediated signalling, and found that the antibody was able to block Ang II-mediated ERK phosphorylation in a dose-dependent manner, in cells expressing both receptors, but not in cells where CB_1R levels were reduced by RNAi-mediated downregulation (Figure 2E); this suggests that the response to Ang II is mediated by the AT1R–CB_1R heteromer.

To further examine if the changes in AT1R signalling in the presence of CB_1R were due to heteromerization and were not the consequence of a cross-talk between downstream signalling cascades, we examined the impact of blocking CB_1R on the G protein coupling to AT1R. [^{35}S]GTPγS-binding experiments indicate that blocking CB_1R with a specific antagonist leads to a decrease in the efficacy of Ang II (Figure 2F). We tested the specificity of the heteromer-mediated signalling by examining if CB_1R activity could regulate the signalling of a non-GPCR, such as PDGFR. Treatment with either two different CB_1R antagonists or with a low concentration of a CB_1R agonist did not affect PDGFbb-mediated ERK phosphorylation (Supplementary Figure S4A and B). We also examined if the increase in Ang II-mediated ERK phosphorylation in the presence of CB_1R could be the result of a non-specific 'presensitization' of the ERK pathway. For this, we stimulated Neuro2A-AT1R cells with a 'subphysiological' dose of PDGFbb and examined the effect on Ang II-mediated ERK phosphorylation. We found that PDGFbb treatment neither altered Ang II-mediated signalling nor rescued this signalling in conditions where CB_1R was blocked with an antagonist (Supplementary Figure S4C). These results exclude the contribution of an alternate mechanism for AT1R–CB_1R cross-talk. Finally, it has been shown for other receptor pairs that, within a heterodimer, the effect of one protomer on the other is bidirectional (Rozenfeld *et al*, 2006). We directly examined this by investigating the changes in CB_1R signalling levels in the presence of an unstimulated AT1R (as we showed that unstimulated CB_1R inhibited AT1R-mediated ERK phosphorylation; Figure 1C and D). Stimulation of CB_1R in Neuro2A cells led to a dose-dependent increase in pERK levels (Figure 2G). This was abolished in the presence of AT1R (in Neuro2A-AT1R cells), but restored when stimulating AT1R with an agonist dose which does not induce a measurable signal (0.01 nM of Ang II) (Figure 2G). This reciprocal regulation of CB_1R signalling by AT1R further supports a heteromer-mediated cross-talk.

Altogether, these results support the notion that the functional interaction between AT1R and CB_1R occurs at the receptor level, through receptor heteromerization.

CB_1R induces a dissociation of the effectors leading to calcium and ERK signalling

In order to explore the specific signalling of the AT1R–CB_1R heteromer, we first investigated the nature of the G protein that is coupled to AT1R (which classically couples to Gαq) in Neuro2A-AT1R cells. Expression of a dominant-negative (DN) Gαq did not lead to a decrease (but led to an unexpected increase) in Ang II-mediated pERK (Figure 3A and C), suggesting that in the context of the AT1R–CB_1R heteromer, AT1R does not couple to Gαq. This is supported by our results showing that expression of DN Gαq under conditions of CB_1R downregulation led to a substantial inhibition of AT1R signalling (Figure 3B and C), indicating that in the absence of CB_1R, AT1R couples to its classical effector, Gαq. These results suggest that in the presence of CB_1R, AT1R uses a different G protein for signalling to the ERK pathway. Next, we examined the involvement of Gαi using pertussis toxin (PTX; that blocks Gαi). This treatment markedly inhibited AT1R signalling (by $>80\%$) only in cells coexpressing CB_1R and AT1R (Figure 3D and F), but not in cells expressing AT1R alone, that is, upon downregulation of CB_1R expression (Figure 3E and F). These results are consistent with the notion that in the presence of CB_1R, AT1R couples to Gαi for signalling to the ERK pathway. We assessed the specificity of this switch in coupling of AT1R by examining the sensi-

 ©2011 European Molecular Biology Organization

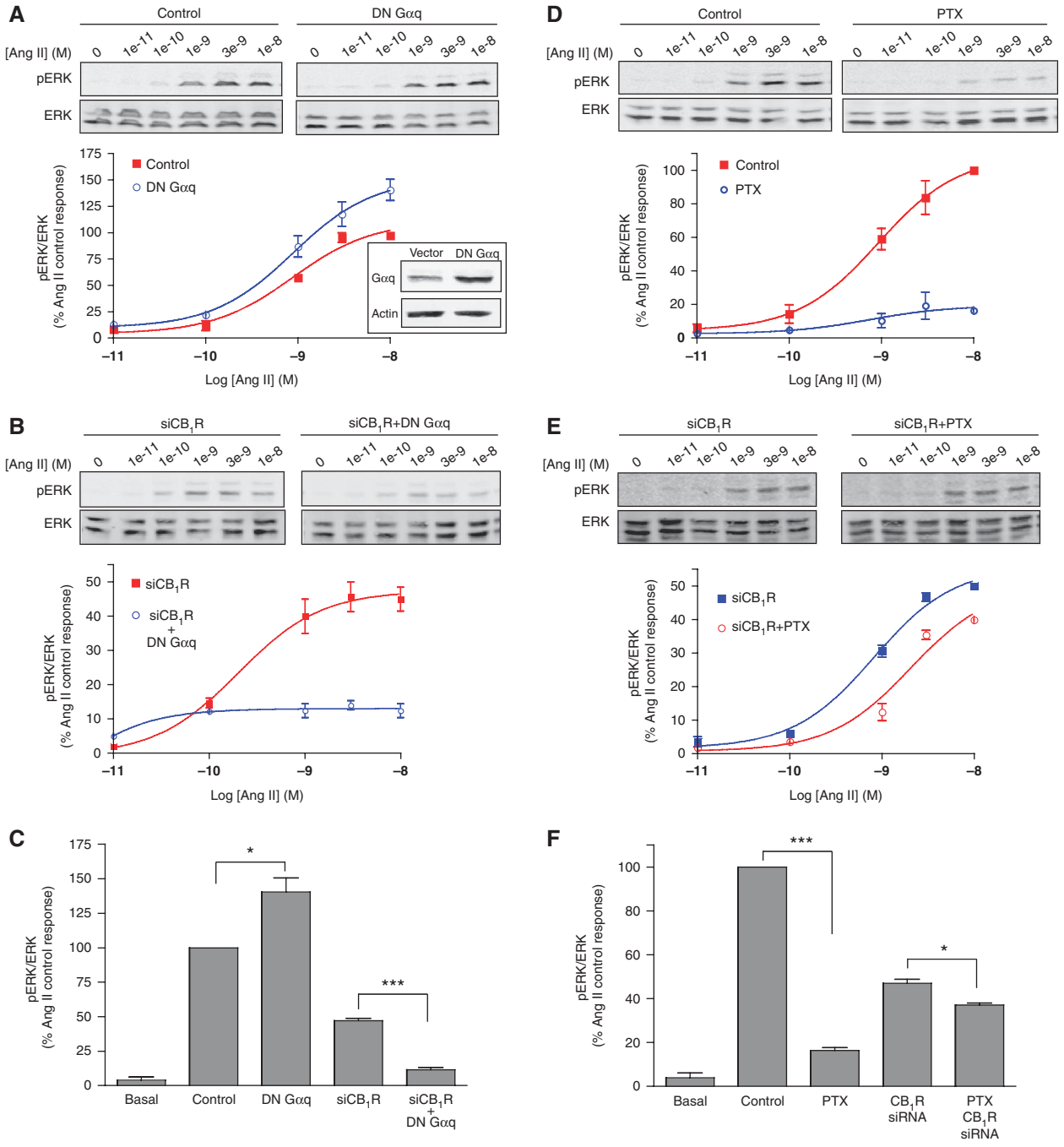

Figure 3 Switch in AT1R G protein coupling to the ERK pathway within the AT1R–CB$_1$R heteromer. Neuro2A-AT1R cells were starved for 4 h and the levels of pERK were measured after various treatments (see below), after 3 min stimulation with 10 nM Ang II. (**A**) Phospho-ERK levels after Ang II stimulation were examined in Neuro2A-AT1R cells, after transfection with a Gαq dominant-negative construct (DN Gαq, see insert). (**B**) Phospho-ERK levels after Ang II stimulation were examined in Neuro2A-AT1R cells transfected with a siRNA to CB$_1$R, after transfection with or without a Gαq dominant-negative construct. (**C**) Data are expressed as the mean ± s.e.m. ($n = 4$ independent experiments). *$P < 0.05$; ***$P < 0.001$. (**D**) Phospho-ERK levels after Ang II stimulation were examined in Neuro2A-AT1R cells after incubation with pertussis toxin (PTX; 15 ng/ml for 16 h). (**E**) Phospho-ERK levels after Ang II stimulation were examined in Neuro2A-AT1R cells transfected with a siRNA to CB$_1$R, after incubation with PTX. (**F**) Data are expressed as the mean ± s.e.m. ($n = 4$ independent experiments). *$P < 0.05$; ***$P < 0.001$.

tivity to PTX of Ang II-mediated ERK phosphorylation, when AT1R was coexpressed with other Gαi-coupled receptors, namely MOR or DOR. We found that PTX prevents Ang II-mediated ERK phosphorylation, only when AT1R is coexpressed with CB$_1$R, but not when expressed alone or with the other Gαi-coupled receptors (Supplementary Figure S4E), supporting the specificity of the switch in G protein coupling to the AT1R–CB$_1$R heteromer.

We then examined if AT1R coupling to Gαi led to inhibition of cAMP production by Ang II treatment. In Neuro2A-AT1R cells, Ang II stimulation led to a dose-dependent inhibition of cAMP production, supporting a coupling to Gαi. This effect was blocked by co-treatment with the CB$_1$R antagonist PF514273 and was markedly decreased upon RNAi-mediated downregulation of CB$_1$R (Figure 4A and C). This regulation of cAMP production by heteromerization was also reciprocal,

©2011 European Molecular Biology Organization

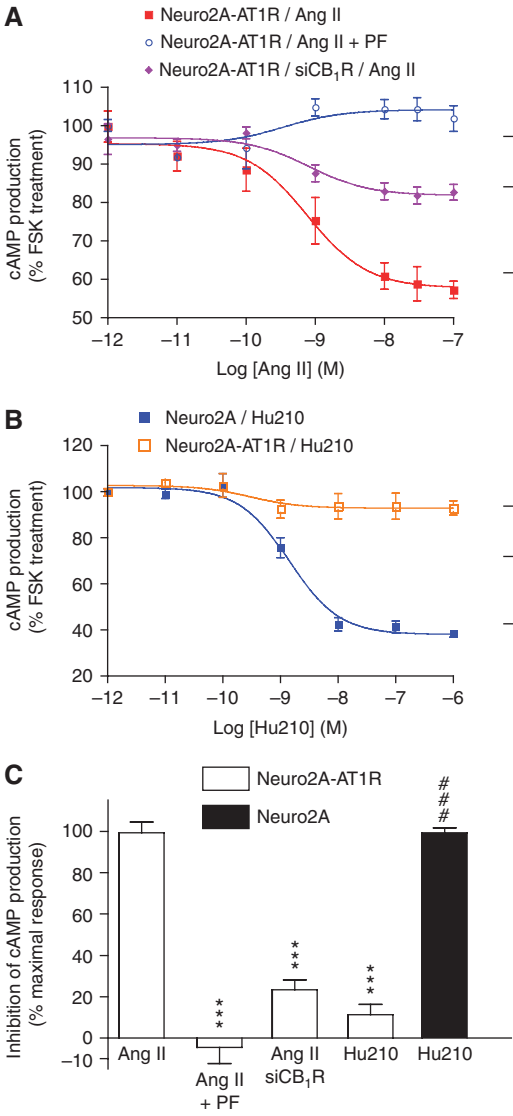

	EC50 (nM)	Emax (% basal)
Ang II	0.8±0.04	57±4
Ang II +PF	0.4+0.01	104±7***
Ang II/siCB$_1$R	0.8±0.02	82±4***

	EC50 (nM)	Emax (% basal)
Neuro2A	1.4±0.02	38±4
Neuro2A-AT1R	0.8+0.01	93±7***

Figure 4 AT1R couples to Gαi within the AT1R–CB$_1$R heteromer. (**A**) Neuro2A-AT1R cells transfected or not with a siRNA to CB$_1$R (siCB$_1$R) in 24-well plates were incubated with increasing concentrations of Ang II in the absence or presence of the CB$_1$R antagonist PF514273 (1 μM) or (**B**) Neuro2A and Neuro2A-AT1R cells in 24-well plates were incubated with increasing concentrations of Hu210 at 37°C for 15 min in the cAMP treatment buffer (0.5 mM isobutylmethylxanthine and 10 μM forskolin in Krebs-Ringer-HEPES buffer). After terminating the reaction by heating at 95°C, cAMP concentrations were determined as described in 'Materials and methods'. Data are expressed as the mean ± s.e.m. ($n=3$ independent experiments). ***$P<0.001$. (**C**) Data are plotted to compare the inhibition of cAMP production across the different experimental conditions. Data are expressed as the mean ± s.e.m. ($n=3$ independent experiments). ***$P<0.001$, indicated conditions versus Ang II; ###$P<0.001$, Hu210 treatment of Neuro2A versus Hu210 treatment of Neuro2A-AT1R.

since the presence of unstimulated AT1R impaired the inhibition of cAMP production induced by the CB$_1$R agonist Hu210 (Figure 4B and C). These experiments confirm that in the context of the AT1R–CB$_1$R heteromer, AT1R couples to Gαi, and that the basal activity of CB$_1$R is required for this pathway.

We next examined if this change in coupling results in further downstream changes in signalling pathway such as those leading to ERK phosphorylation. While the PKC inhibitor calphostin C attenuated Ang II-mediated ERK phosphorylation in cells where CB$_1$R was downregulated, it had no effect on Ang II-mediated ERK phosphorylation in Neuro2A-AT1R cells (Supplementary Figure S5A). We also found that PLC is involved in Ang II-mediated ERK phosphorylation irrespective of the presence of CB$_1$R. These suggest a dissociation between PLC and PKC for Ang II-mediated pERK in CB$_1$R-expressing cells, in agreement with previous reports (Ma'ayan *et al*, 2009). In addition, we found a switch in the role of Arrestin3 in the regulation of ERK signalling upon heteromerization of AT1R with CB$_1$R; while, as previously described, Arrestin3 contributes to Ang II-mediated ERK phosphorylation (Ahn *et al*, 2004; Supplementary Figure S5B), in the presence of CB$_1$R, downregulation of Arrestin3 leads to an increase in pERK, indicating a role for Arrestin3 in the desensitization of AT1R within the heteromer (Supplementary Figure S5B).

We also examined if signalling events classically mediated by AT1R, namely the mobilization of calcium from intracellular stores via a mechanism mediated by coupling to Gαq, were altered in the context of the AT1R–CB$_1$R heteromer.

©2011 European Molecular Biology Organization

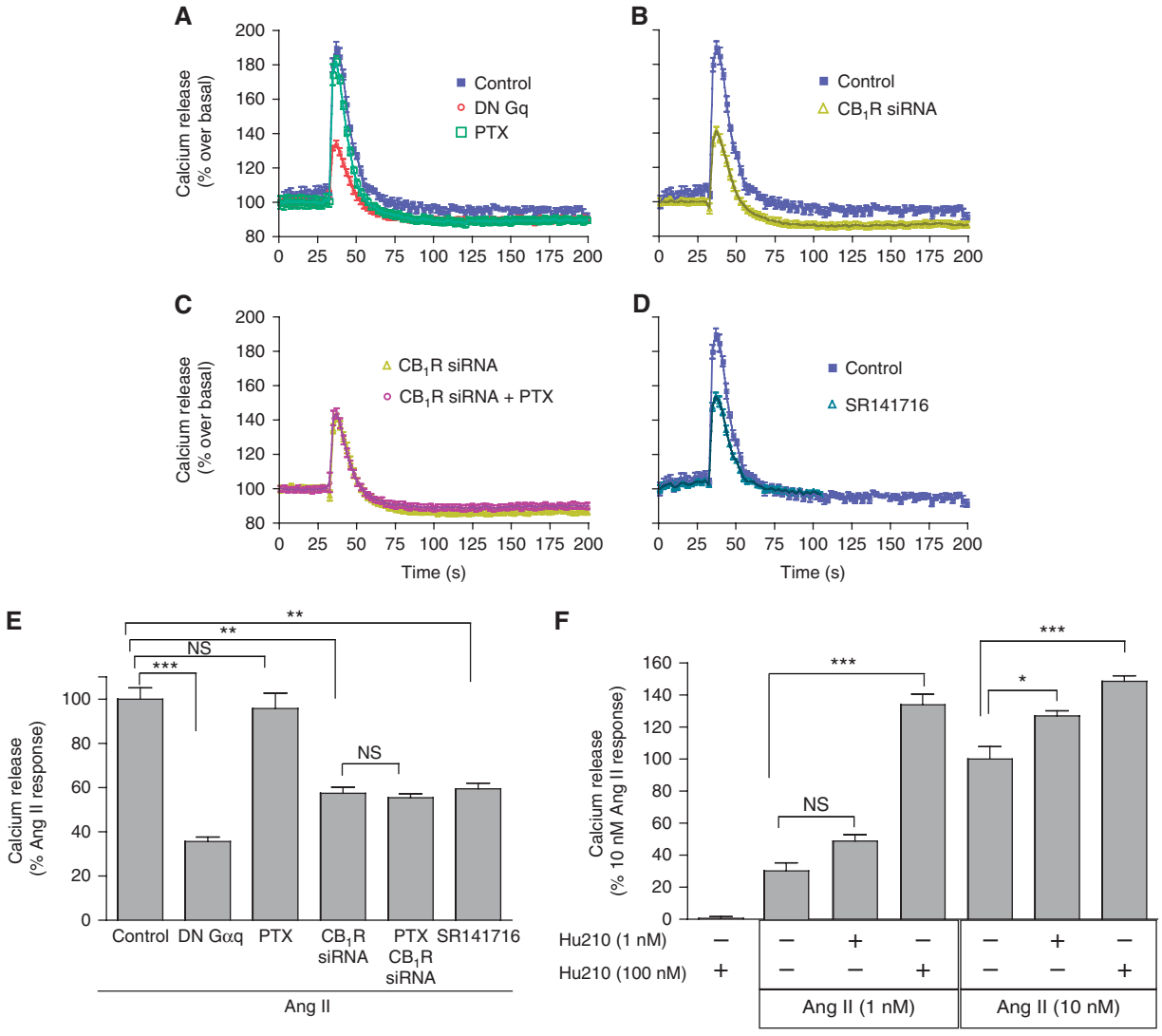

Figure 5 Regulation of Ang II-mediated calcium signalling by CB_1R. (**A**) Neuro2A-AT1R cells were transfected without or with a DN Gαq plasmid and treated or not with PTX (50 ng/ml). The relative levels of intracellular Ca^{2+} release were measured for 200 s. (**B**) Neuro2A-AT1R cells were transfected without or with siRNA to CB_1R and stimulated with Ang II (10 nM). The relative levels of intracellular Ca^{2+} release were measured for 200 s. (**C**) Neuro2A-AT1R cells were transfected with siRNA to CB_1R, treated or not with PTX (50 ng/ml), and stimulated with Ang II (10 nM). The relative levels of intracellular Ca^{2+} release were measured for 200 s. (**D**) Neuro2A-AT1R cells were stimulated with Ang II (10 nM) in the absence or presence of SR141716 (1 μM). The relative levels of intracellular Ca^{2+} release were measured for 200 s. (**E**) Intracellular Ca^{2+} levels correspond to fold increase over basal and are plotted as percent response obtained with Ang II treatment. Data are expressed as the mean ± s.e.m. ($n = 3$ independent experiments in quintuplicate). $^{**}P < 0.01$; $^{***}P < 0.001$; NS, non-significant. (**F**) Intracellular Ca^{2+} levels measured after treatment of Neuro2A-AT1R with Hu210 and Ang II, alone or in combination, correspond to fold increase over basal and are plotted as percent response obtained with 10 nM Ang II treatment. Data are expressed as the mean ± s.e.m. ($n = 3$ independent experiments in quintuplicate). $^{*}P < 0.05$; $^{***}P < 0.001$; NS, non-significant.

Stimulation of heteromer expressing cells with Ang II led to a marked increase in intracellular calcium levels (Figure 5A; Supplementary Figure S6C). This was largely prevented by expression of DN Gαq (by ~60%), but was not affected by treatment with PTX (Figure 5A and E), indicating that Ang II stimulation leads to a Gαq-mediated increase in intracellular calcium concentration. RNAi-mediated CB_1R downregulation led to a decrease (by ~50%) of this signalling response (Figure 5B and E), which was not affected by PTX treatment (Figure 5C), suggesting that CB_1R contributes to Ang II signalling by the Gαq pathway. This is supported by our results showing that treatment with the CB_1R-specific antagonist SR141716 also led to a decrease (~50%) of Ang II-mediated increase in intracellular calcium concentration (Figure 5D and E). In contrast, CB_1R stimulation with Hu210 did not lead to an increase in intracellular calcium levels in either Neuro2A or Neuro2A-AT1R cells in the absence of concomitant stimulation of AT1R (Figure 5F; Supplementary Figure S6A and B). However, Hu210 was able to potentiate Ang II-mediated signalling (Figure 5F; Supplementary Figure S6D and E), supporting our previous results that CB_1R activation enhances AT1R activity.

In control experiments, we examined the influence of other Gαi-coupled receptors on AT1R-mediated Gαq signalling. We observed that co-stimulation of MOR with its agonist DAMGO, but not co-stimulation of DOR with its agonist deltorphin was potentiating Ang II response

©2011 European Molecular Biology Organization

(Supplementary Figure S4E). These results further support the specificity of the functional interaction between CB_1R and AT1R, affecting both Gαi- and Gαq-mediated responses, as opposed to interactions between MOR and AT1R that affect only Gαq-mediated response, and the absence of measurable functional interaction between DOR and AT1R.

Taken together with the finding that Ang II-mediated ERK phosphorylation is via the Gαi/o-mediated pathway, these results indicate that AT1R–CB_1R heteromer recruits both Gαq (to mediate calcium signalling) and Gαi (to mediate ERK signalling), and that signalling via both these G proteins is controlled by CB_1R activity, and enhanced by CB_1R basal activation. Hence, AT1R–CB_1R heteromer functions as a signal integrator and enhances the repertoire of AT1R and CB_1R signalling.

CB_1R interacts with AT1R in activated HSCs

Activation of HSCs is the dominant event in liver fibrogenesis and proceeds along a continuum that involves progressive changes in cellular function. Activated HSCs produce excess extracellular matrix proteins, including collagens, resulting in fibrosis (Friedman, 2008). Cannabinoid receptors exhibit marginal expression in the normal liver but an enhanced expression in the fibrotic human liver, predominantly in activated HSCs (Teixeira-Clerc *et al*, 2006). CB_1R contributes to fibrogenesis, since administration of the CB_1R antagonist rimonabant (SR141716) or genetic ablation of CB_1R inhibits fibrosis progression in three models of chronic liver injury (namely, CCl4-, thioacetamide-, and bile duct ligation-induced fibrosis) (Teixeira-Clerc *et al*, 2006). However, the molecular mechanism by which CB_1R promotes HSC activation and liver fibrosis are not understood. Given the potentiation of Ang II signalling by heteromerization of AT1R with CB_1R, and the profibrogenic properties of hyperreactive AT1R (Billet *et al*, 2008), we hypothesized that upregulated CB_1R could interact with AT1R, a resident receptor in HSCs and facilitate AT1R profibrogenic activity.

First, we examined the relative abundance of AT1R and CB_1R in HSCs from control rats (cHSCs) or rats treated with ethanol for 8 months (eHSCs) (see details in 'Materials and methods'). Activation of the eHSCs was supported by a substantial increase in the levels of α-smooth muscle actin (α-SMA), a marker of HSC activation (Figure 6A). We found that CB_1R was markedly upregulated (~7-fold) and AT1R was modestly upregulated (~1.5-fold) in eHSCs compared with cHSCs (Figure 6A). Similar changes in receptor expression were measured by radioligand binding (Table I). These results indicate that chronic ethanol treatment leads to upregulation of CB_1R in HSCs, in agreement with the upregulation of CB_1R observed in other models of liver injury (Teixeira-Clerc *et al*, 2006).

Next, we examined direct interaction between CB_1R and AT1R in these cells and found that CB_1R could be detected in the AT1R immunoprecipitate only from activated but not from control HSCs (Figure 6B), supporting heteromerization of AT1R–CB_1R specifically in activated HSCs. Using the AT1R–CB_1R heteromer-selective antibody, we found substantial AT1R–CB_1R immunoreactivity in activated HSCs but not

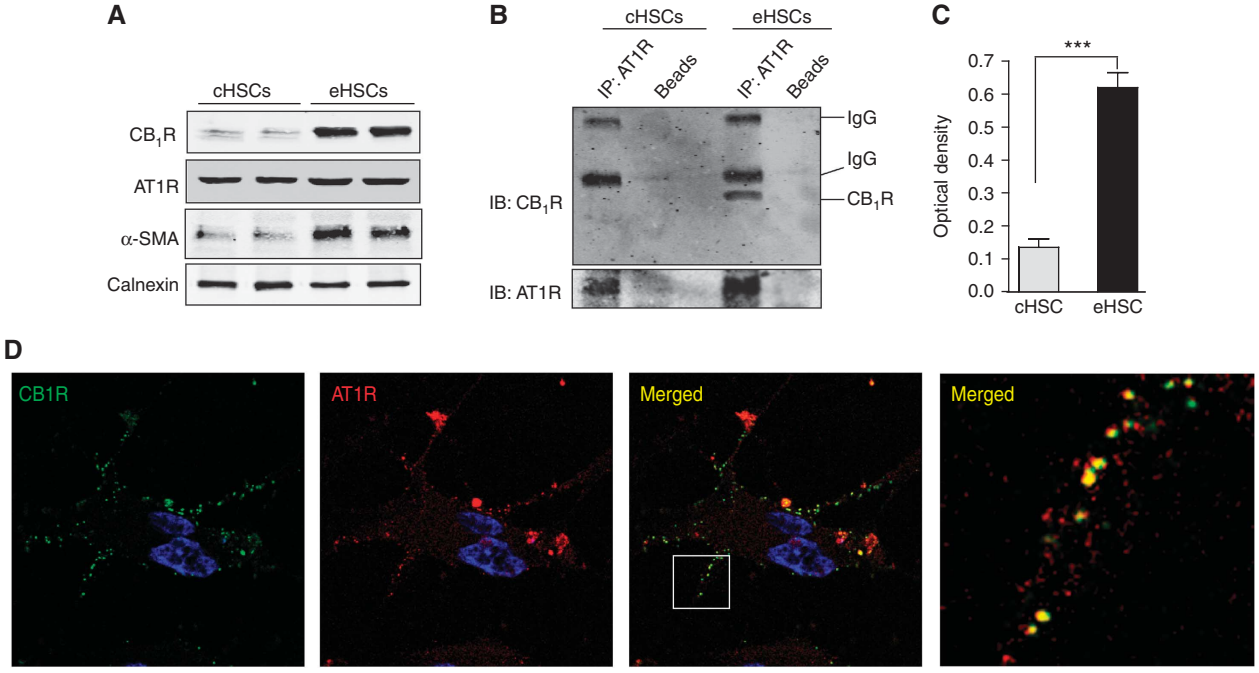

Figure 6 Presence of AT1R–CB_1R heteromers in activated HSCs. (**A**) Expression levels of CB_1R, AT1R, and α-SMA by western blotting analysis in HSCs from control (cHSC) and ethanol (eHSCs) treated rats. Calnexin is used as a loading control. (**B**) Association of AT1R and CB_1R in eHSCs. Lysates from cHSCs and eHSCs were subjected to immunoprecipitation using an anti-AT1R antibody (1 μg)/protein A/G agarose, and to western blotting analysis with CB_1R antibody (1:500). CB_1R is detected in the AT1R immunoprecipitate from eHSCs (and not cHSCs). (**C**) Detection of AT1R–CB_1R heteromers with heteromer-selective monoclonal antibodies. Receptor abundance was determined in cHSCs and eHSCs with a monoclonal antibody to AT1R–CB_1R by ELISA. Results represent the means ± s.e.m. obtained with antibodies from seven different hybridoma clones. $^{***}P<0.001$. (**D**) Colocalization of AT1R and CB_1R in activated HSCs. eHSCs grown on coverslips were fixed with 4% PFA, permeabilized with 0.1% Triton X-100, and stained with primary rabbit polyclonal anti-CB_1R (1:500) and goat polyclonal anti-AT1R (1:200) antibodies. After fluorescent secondary antibody staining, the coverslips were mounted with mowiol. Slides were examined with a Leica SP5 confocal microscope.

©2011 European Molecular Biology Organization

in HSCs from control rats (Figure 6C), supporting higher levels of AT1R–CB_1R heteromer in activated HSCs. Finally, CB_1R and AT1R were colocalized at the cell surface of the activated HSCs, in agreement with their presence in heteromeric complexes (Figure 6D).

Table I Receptor expression levels in Neuro2A-AT1R, eHSC, and cHSC as determined by radioligand binding as described in 'Materials and methods'

	CB_1R	AT1R
Neuro2A-AT1R	185 ± 15	232 ± 20
eHSC	207 ± 44	215 ± 35
cHSC	7 ± 3	121 ± 28

Results are expressed in fmol receptor/mg protein, as the mean ± s.e.m. ($n = 3$ independent experiments).

CB_1R activity governs Ang II-mediated signalling in activated HSCs

Next, we examined if in HSCs, AT1R was hyperreactive and if CB_1R had a role in this response. Treatment with Ang II led to a marked increase in pERK levels in activated HSCs (Figure 7A and B) above the level seen in control HSCs (Figure 7C and D). This increase in signalling was dependent on CB_1R since treatment with a CB_1R-specific antagonist as well as blocking the formation of the endocannabinoid 2-AG with THL blocked Ang II response in activated HSCs (Figure

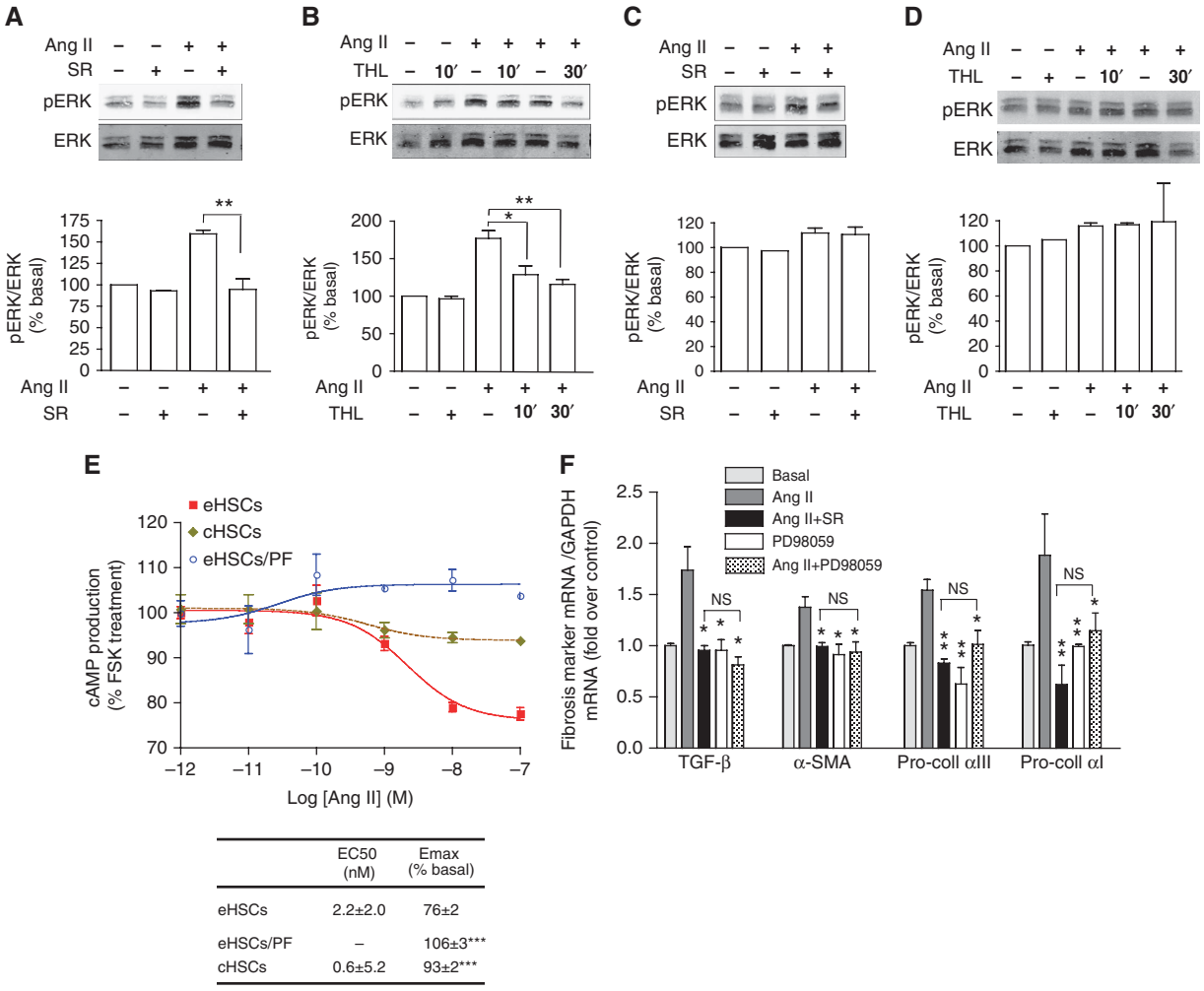

	EC50 (nM)	Emax (% basal)
eHSCs	2.2±2.0	76±2
eHSCs/PF	–	106±3***
cHSCs	0.6±5.2	93±2***

Figure 7 Regulation of AT1R responses by CB_1R in activated HSCs. (**A**) eHSCs were stimulated for 10 min with 1 μM Ang II in the absence or presence of SR141716 (SR, 1 μM) and the levels of pERK and ERK examined as described in 'Materials and methods'. Data are expressed as the mean ± s.e.m. ($n = 3$ independent experiments). $^{**}P < 0.01$. (**B**) eHSCs were treated with THL (1 μM, for 0, 10, or 30 min) before treatment with Ang II (1 μM). Data are expressed as the mean ± s.e.m. ($n = 3$ independent experiments). $^{*}P < 0.05$; $^{**}P < 0.01$. (**C**) cHSCs were stimulated for 10 min with 1 μM Ang II in the absence or presence of SR141716 (SR) and the levels of pERK and ERK examined as described in 'Materials and methods'. (**D**) cHSCs pretreated with THL for 10 or 30 min were stimulated with 1 μM Ang II. Lysates were subjected to SDS–PAGE and immunoblotting. The levels of Ang II-mediated pERK normalized to total ERK are indicated. Data are expressed as the mean ± s.e.m. ($n = 3$–4 independent experiments). (**E**) eHSCs and cHSCs in 24-well plates were incubated with increasing concentrations of Ang II in the absence or presence of the CB_1R antagonist PF514273 (1 μM) at 37°C for 15 min in the cAMP treatment buffer (0.5 mM isobutylmethylxanthine and 10 μM forskolin in Krebs-Ringer-HEPES buffer). After terminating the reaction by heating at 95°C, cAMP concentrations were determined as described in 'Materials and methods'. Data are expressed as the mean ± s.e.m. ($n = 3$ independent experiments). $^{***}P < 0.001$. (**F**) eHSCs were stimulated with Ang II (1 μM) in the absence or presence of SR141716 (SR, 1 μM) or of PD98059 (MEK inhibitor, 10 μM) for 4 h before the RNA was harvested. After reverse transcription, the number of copies of mRNA for the indicated transcripts were determined by real-time PCR. Data were normalized to GAPDH mRNA and are expressed as the mean ± s.e.m. ($n = 3$ in quadruplicate). $^{*}P < 0.05$; $^{**}P < 0.01$ (versus Ang II treatment); NS, non-significant (Ang II + PD98059 versus Ang II + SR).

©2011 European Molecular Biology Organization

7A and B) but not in control HSCs (Figure 7C and D). These results are consistent with the idea that CB_1R and the endocannabinoid tone control the signalling of AT1R in the context of AT1R–CB_1R heteromers present in activated HSCs.

We also examined if AT1R couples to Gαi in the presence of CB_1R in HSCs. In activated HSCs, Ang II treatment led to a dose-dependent inhibition of cAMP production (Figure 7E). Blockade of this effect by the CB_1R antagonist PF514273 as well as absence of inhibition of cAMP levels in control HSCs (that do not express CB_1R), support a role for heteromerization with CB_1R in facilitating the coupling of AT1R to Gαi in activated HSCs.

Modulation of AT1R profibrogenic activity by CB_1R

Next, we examined if we could target the AT1R–CB_1R heteromer to block Ang II-mediated HSC activation. In activated HSCs, we found that stimulation of AT1R led to an increase in expression of the profibrogenic markers α-SMA, TGF-β, pro-collagen αIII, and pro-collagen αI by as much as 120–160% over baseline; this increase could be completely blocked by treatment with the CB_1R antagonist SR141716, or with the MEK inhibitor PD98059 (Figure 7F), indicating that the profibrogenic potential of AT1R requires CB_1R activity and that CB_1R–AT1R heteromer could represent a novel disease-specific therapeutic target.

Discussion

In this study, we show that when coexpressed, CB_1R and AT1R physically and functionally interact in recombinant as well as in endogenous systems. Interaction with CB_1R confers new signalling properties to AT1R including a change in G protein coupling, and enhanced responsiveness to Ang II. This mechanism allows for a regulation of AT1R responses by CB_1R expression levels, underscoring the relevance of CB_1R upregulation during chronic diseases on the function and properties of other coexpressed receptors.

Cross-talk between Gαi- and Gαq-coupled receptors has been described for several receptor pairs, and typically leads to a potentiation of Gαq signalling (Carroll *et al*, 1995; Hilairet *et al*, 2003; Rives *et al*, 2009), found often to be heteromerization independent (Rives *et al*, 2009). However, other studies have convincingly reported heteromerization-dependent cross-talk between Gαi- and Gαq-coupled receptors, either involving a class A and a class C receptors (Gonzalez-Maeso *et al*, 2008) or two class A receptors (Breit *et al*, 2006). In the present study, using a variety of methods such as co-immunoprecipitation, BRET assays, heteromer-selective antibody detection, and changes in receptor subcellular localization, we demonstrate physical interactions between two class A GPCRs, AT1R, and CB_1R.

While the cross-talk between Gαi- and Gαq-coupled receptors involving class C GPCRs has been shown to lead to a potentiation of the Gαq-mediated pathway, AT1R–CB_1R heteromerization appears to lead to a more complex scenario. In addition to a potentiation of the Gαq-mediated signalling, as measured by an increase in Ang II-mediated calcium response by CB_1R basal activity (and by CB_1R agonist stimulation), heteromerization with CB_1R also potentiates a Gαi-mediated mitogenic signalling in response to Ang II. This coupling to Gαi, confirmed by sensitivity to PTX and by the inhibition of cAMP production, suggests a unique signalling property of the receptor complex that differs from the cross-talk between Gαi- and Gαq-coupled receptors involving class C GPCRs (Rives *et al*, 2009). This mechanism is also different from that of the sensory neuron-specific receptor-4 (SNSR-4)–DOR heteromer for which concomitant activation of the Gαi-coupled DOR and Gαq-coupled SNSR-4 led to the inhibition of the Gαi signalling and full activation of the Gαq-mediated phospholipase C pathway (Breit *et al*, 2006).

The potentiation of AT1R signalling by heteromerization with CB_1R results in the enhancement of the mitogenic signalling and profibrogenic activity of AT1R. Using a transgenic mouse harbouring a hyperreactive mutant of AT1R, that exhibits enhanced signalling in response to Ang II, it was demonstrated that hyperreactivity of AT1R can be responsible for deleterious, in particular profibrogenic, effects of Ang II (Billet *et al*, 2007). However, no such 'gain of function' mutations of AT1R within its coding region have been identified (Davies *et al*, 1997; Sachse *et al*, 1997), suggesting that alternative molecular mechanisms could be responsible for the 'gain of function'-like phenotype of AT1R in diseases. We propose that association with CB_1R is sufficient to confer hyperreactivity to AT1R. We find that basal activity of CB_1R enhances Ang II-mediated signalling, and that blocking CB_1R leads to a decrease in AT1R responsiveness to Ang II, suggesting that CB_1R within the AT1R–CB_1R heteromer, confers a 'gain of function'-like hyperreactive property to AT1R, underscoring the relevance of AT1R–CB_1R heteromerization in pathology.

Mechanisms of cross-talk between AT1R and CB_1R, at both the transcriptional and signalling levels, have been reported. CB_1R activity has been involved in regulating AT1R expression in endothelial cells (Tiyerili *et al*, 2010) and AT1R has been involved in regulating the activity of the endocannabinoid biosynthetic enzyme DAGL (Turu *et al*, 2007). This latter study elegantly demonstrated that activation of AT1R leads to a Gαq-mediated increase in intracellular calcium, which in turn activates the calcium-dependent DAGL, leading to increased production of 2-AG, resulting in enhanced basal activity of CB_1R (Turu *et al*, 2007). While these studies demonstrate indirect cross-regulation between CB_1R and AT1R, to date, mechanisms involving direct protein–protein interaction between these two receptors affecting their function had not been explored. In the present study, we demonstrate the regulation of AT1R by CB_1R through receptor heteromerization. The hyperreactivity of AT1R described herein cannot be the consequence of transcriptional regulation of its expression, since expression or abundance of AT1R are not significantly changed in the presence of CB_1R, in any of the models used. Furthermore, the alteration of AT1R properties by CB_1R occurs in endogenous systems as well as in heterologous cells (where transfected AT1R is not subject to transcriptional regulation). In addition, the hyperreactivity of AT1R described herein does not involve the regulation of DAGL activity by AT1R, since directly blocking CB_1R with a specific antagonist prevents Ang II-mediated signalling. In addition, the reciprocity of the regulation of receptor activity by heteromerization (i.e., the functional inhibition of CB_1R activity by AT1R) further confirms the absence of effect of DAGL activity on our observations. Taken together, our studies strongly support AT1R–CB_1R heteromerization as a mechanism for the altered properties of AT1R.

 ©2011 European Molecular Biology Organization

Our finding that AT1R–CB_1R heteromerization facilitates profibrogenic signalling, together with the possibility of auto and paracrine transactivation of CB_1R by AT1R (described above), suggest complementary mechanisms that converge towards upregulation of profibrogenic stimulation.

Another important finding in this study is that the basal activity of CB_1R is sufficient to enhance the activity of associated AT1Rs underscoring a particularly important role for the endocannabinoid tone in the maintenance of fibrosis. It is likely that this mechanism of 'hijacking' of receptor activity by the upregulated CB_1Rs has a role in additional pathologies, particularly in the case of metabolic syndrome where CB_1R expression is increased in select tissues (Kunos *et al*, 2008). One could propose that, as seen in activated HSCs, CB_1R could interact with AT1R in hepatocytes and adipocytes where CB_1R expression is increased during disease (Bensaid *et al*, 2003; Jeong *et al*, 2008). The generalization of this mechanism is further supported by the observation that in the presence of CB_1R, orexin receptor-mediated signalling was enhanced and found to be PTX sensitive and could be blocked by a CB_1R antagonist (Hilairet *et al*, 2003).

Previous studies exploring the role of GPCR heteromers in disease (AbdAlla *et al*, 2001, 2005) have led to the proposal that upregulated heteromers during pathologies represent potential drug targets (Rozenfeld *et al*, 2006). The evidence for disease-specific AT1R–CB_1R receptor interaction further suggests that this complex could represent a novel drug target for anti-fibrotic compounds, allowing selective peripheral targeting of CB_1R, and thereby preventing the psychoactive effects of CB_1R antagonists (Kunos *et al*, 2009).

Materials and methods

Cell lines, reagents, and plasmids

Human embryonic kidney (HEK)-293 and Neuro2A cells from ATCC were maintained in DMEM + 10% FBS at 37°C in a humidified 5% CO_2 incubator. HSCs were maintained in DMEM/F12 50% (v/v) + 10% FBS. Rabbit monoclonal anti-phospho-ERK and mouse monoclonal anti-ERK antibodies were from Cell Signaling Technology Inc. Polyclonal anti-Calnexin, monoclonal anti-Flag antibodies, PTX, and THL were from Sigma. Rabbit and goat polyclonal anti-AT1R, polyclonal anti-Gαq, polyclonal anti-HA antibodies, protein A agarose-coupled anti-CB_1R antibody, CB_1R and control siRNAs, and coelenterazine A were from Santa Cruz Biotechnology. Rabbit polyclonal anti-CB_1R antibody used for western blotting was from Cayman Chemicals, and rabbit polyclonal anti-CB_1R antibody used for immunostaining was a gift from Dr Ken Mackie (University of Indiana). Monoclonal anti-α-SMA antibody was from Abcam. The secondary antibodies IRDye 680-labelled anti-rabbit antibody, IRDye 800-labelled anti-mouse, and anti-goat antibodies were from Rockland Immunochemicals (Gilbertsville, PA). Hu210, Ang II, and PF514273 were from Tocris Bioscience. SR141716 was from NIDA drug support program. DN Gαq (Q209L/D277N) plasmid was a gift from Dr Ken Mackie (University of Indiana).

HSC isolation

HSCs from ethanol-treated rats were generated as described (Cubero and Nieto, 2008). Rats (300 g female Sprague-Dawley, $N = 10$/group) were fed the control or ethanol Lieber-DeCarli diets for 8 months (Lieber and DeCarli, 1989). Animals received humane care according to the criteria outlined in the Guide for Care and Use of Laboratory Animals. Details regarding pathology of the liver of the control and alcohol-fed rats are described in Cubero and Nieto (2008) and Urtasun *et al* (2009). Briefly, haematoxylin and eosin staining showed microvesicular and macrovesicular steatosis in livers from ethanol-fed rats; transaminases and non-esterified fatty acids were elevated two-fold and six-fold, respectively, in the ethanol-fed rats.

Plasmid and siRNA transfections were carried out as described (Rozenfeld and Devi, 2007).

Co-immunoprecipitation and western blotting

Cells were lysed for 1 h in lysis buffer (1% Triton, 150 mM NaCl, 1 mM EDTA, 1 mM EGTA, and 50 mM Tris–Cl, pH 7.4) containing protease inhibitor cocktail (Sigma). For immunoprecipitation, cell lysates containing 400–600 μg of protein were incubated with the anti-AT1R antibody (1 μg)/protein A/G agarose complex or with a protein A agarose-coupled anti-CB_1R antibody (1 μg) overnight at 4°C. The beads were washed three times with lysis buffer and once with the same buffer without detergent. Proteins were eluted in 60 μl of 2× Laemmli buffer containing 1% 2-mercaptoethanol. Proteins were resolved by 10% SDS–PAGE, and subjected to western blotting as described (Rozenfeld and Devi, 2008).

Immunofluorescence and confocal microscopy was carried out as described (Rozenfeld and Devi, 2008). Slides were visualized with a Leica TCS SP5 confocal microscope. Images were acquired with ×63/1.32 PL APO objective lens, and analysed in sequential scanning mode.

Western blot and phospho-ERK assays were carried out as described in the case of experiments with Neuro2A cells (Rozenfeld and Devi, 2008). In all cases, the cells were starved at least 4 h before the treatments. For experiments with HSCs, freshly plated cells were stimulated for 10 min with 1 μM Ang II in the presence or absence of SR141716 or THL (as indicated). Phospho-ERK and ERK were detected with rabbit monoclonal anti-phospho-p44/42 MAPK (anti-pERK, 1:1000) and mouse monoclonal anti-p44/42 MAPK (anti-ERK, 1:1000) antibodies. Both blotting and imaging with the Odyssey imaging system (LI-COR, Lincoln, NE) were performed following the manufacturer's protocols. The secondary antibodies that were used included: IRDye 680-labelled anti-rabbit antibody, IRDye 800-labelled anti-mouse, and anti-goat antibodies (1: 10 000).

Subtractive immunization

For induction of tolerance to immunogenic epitopes in Neuro2A cell membranes, female balb/c mice (6–8 weeks old, 25–35 g body weight) were injected intraperitoneally (i.p.) with 5 mg/kg Neuro2A cell membranes and 15 min later with cyclophosphamide (100 mg/kg body weight, i.p.). The cyclophosphamide injection was repeated after 24 and 48 h, respectively. Mice were bleed every 15 days and antibody titres checked by ELISA against Neuro2A cell membranes. This protocol was repeated at 2-week intervals until stable background titres were obtained with Neuro2A cell membranes. Mice were then given an i.p. injection of membranes from Neuro2A cell expressing AT1R (in addition to CB_1R endogenously expressed) (5 mg/kg) in complete Freund's adjuvant. Booster i.p. injections of Neuro2A cell membranes expressing AT1R were administered every 15 days. Antibody titres were checked by ELISA against Neuro2A cell membranes from untransfected cells and from cells expressing AT1R, as described for MOR–DOR (Gupta *et al*, 2010). Spleens from animals giving a high titre with Neuro2A cell membranes expressing AT1R receptors were fused with SP-20 myeloma cells to generate monoclonal antibodies as described. Clones secreting monoclonal antibodies were screened by ELISA against untransfected Neuro2A cell membranes, and HEK293 membranes expressing AT1R or Neuro2A cell membranes expressing AT1R using 1:10 hybridoma supernatant and 1:500 horseradish peroxidase labelled anti-mouse IgG.

ELISAs were carried out as previously described (Gupta *et al*, 2007) with cells (2×10^5/well) expressing individual receptors or with cells coexpressing AT1R and CB_1R, or the indicated GPCRs.

[^{35}S]GTPγS binding

Membranes from Neuro2A-AT1R cells were prepared by homogenization in ice-cold 50 mM Tris–Cl buffer pH 7.4 containing 1 mM EDTA and 10% sucrose. The membranes were incubated with increasing concentrations of Ang II ± PF514273 (1 μM) in the presence of 100 μM GDP and 0.1 nM [^{35}S]GTPγS. Basal binding was determined in the presence of GDP and absence of agonist and cold GTPγS. Non-specific binding was determined by adding 10 mM GTPγS to a parallel set of tubes.

©2011 European Molecular Biology Organization

Measurement of intracellular cAMP levels

Cells in 24-well plates were incubated with increasing concentrations of Ang II ± PF514273 (1 μM) in 250 μl of treatment buffer (0.5 mM isobutylmethylxanthine and 10 μM forskolin) in Krebs-Ringer-HEPES buffer (KRHB; 110 mM NaCl, 25 mM glucose, 55 mM sucrose, 10 mM HEPES, 5 mM KCl, 1 mM $MgCl_2$, 1.8 mM $CaCl_2$, pH 7.4). The cells were incubated at 37°C for 15 min. The reaction was terminated by heating the cells at 95°C for 10 min. The cAMP level in the supernatant was measured using the Parameter Cyclic AMP Assay (R&D Systems), as per manufacturer's recommendation.

Intracellular calcium release was carried out as described (Gomes *et al*, 2009). Briefly, Neuro2A or Neuro2A-AT1R cells were plated onto poly-L-lysine-coated 96-well clear-bottom plates (40 000 cells/well). On the next day, the growth medium was removed, and cells were washed twice in HBSS buffer containing 20 mM HEPES. Cells were incubated with Fluo-4 NW calcium dye (3 μM in 100 μl) for 1 h at 37°C. The different compounds were added to the wells by the robotic arm of the FLEX Station, and intracellular Ca^{2+} levels were measured for 200 s at excitation 494 nm and emission 516 nm. In experiments examining the effect of PTX, cells were incubated with 50 ng/ml PTX for 6 h, and maintained in the presence of PTX during the different incubation phases and ligand stimulation.

BRET assays were carried out as described (Pignatari *et al*, 2006). Briefly, HEK293 cells were transfected with CB_1R–Luc alone, or with AT1R–eGFP in the absence or presence of untagged AT1R or ECE-2, or with MOR–Luc with AT1R–eGFP and BRET measured as described.

Real-time quantitative reverse transcription–PCR

Total RNA was isolated from 3×10^8 HSCs using the TRIzol method (Invitrogen, Carlsbad, CA, USA). RNA (1.0 μg) was reverse transcribed in 20 μl of buffer containing 50 μM oligo(dT)20, 25 mM $MgCl_2$, 0.1 M dithiothreitol, 40 U/μl RNaseOUT, and 200 U/μl SuperScript III RT for 50 min at 50°C. The reaction was stopped by incubating the samples at 85°C for 5 min and 40 μl of nuclease-free water was added. Real-time PCR was performed by using the Brilliant SYBR Green QPCR Master Mix. The PCR template source was either 30 ng of first-strand cDNA or purified DNA standard. Amplification was performed with a spectrofluorometric thermal cycler (Stratagene). After an initial denaturation step at 95°C for 10 min, amplification was performed using 40 cycles of denaturation (95°C for 30 s), annealing (56°C for 1 min), and extension (72°C for 1 min). To standardize mRNA levels, we amplified GAPDH, a housekeeping gene, as an internal control. Gene expression was normalized by calculating the ratio between the number of cDNA copies of collagen type I, type III, TGF-β, α-SMA, and that of GAPDH.

Radioligand binding

Membranes from the indicated cell lines (10 μg for [^{125}I]Ang II binding and 50 μg for [^{3}H]CP55940 binding) were incubated with [^{125}I]Ang II (2200 Ci/mmol, Perkin-Elmer, Boston, MA, USA) in the absence or presence of unlabelled Ang II (Tocris), or with [^{3}H]CP55940 (77.5 Ci/mmol, NIDA, USA) in the absence or presence of unlabelled PF514273 (Tocris). Non-specific binding was defined as the amount of radioligand binding in the presence of 10 μM Ang II or 10 μM PF514273. Membrane bound radioactivity was quantified on a γ counter (Wallac Wizard 1470 Automatc gamma counter, Perkin-Elmer) or a β counter (Beckman LS-5000 TD, USA). Ligand-binding data were analysed using GraphPad Prism software (GraphPad Software, San Diego, USA). All measurements were carried out in triplicate in three independent experiments.

Statistical analyses

Statistical significance and *P*-values were determined by the Student's *t*-test when comparing two groups, or by one-way ANOVA with Bonferroni post-test when comparing multiple groups, using the GraphPad Prism software (GraphPad Software). *P*-value ($^*P<0.05$; $^{**}P<0.01$; $^{***}P<0.001$) of <0.05 was considered statistically significant.

Supplementary data

Supplementary data are available at *The EMBO Journal* Online (http://www.embojournal.org).

Acknowledgements

We thank Drs Scott Friedman and Arthur Cederbaum for constructive discussions and comments, Dr Ken Mackie for the gift of the CB_1R antibody and DN Gq plasmid, Drs Emeline Maillet and Mariana Max for the use of the Flex Station II. This work was supported by NIH grants DA08863, DA19521, and 1P50GM071558 (to LAD); DK069286 and AA017733 (to NN); AA017067 (to NN and RR); and R24 CA095823 (to MSSM-Microscopy Shared Resource Facility).

Author contributions: RR and LAD designed the experiments and wrote the paper. RR planed and performed the experiments and analysed the data. AG developed the heteromer-specific antibodies. AG, KG, MPL, DLR, and IG carried out experiments. NN contributed cell lines and reagents.

Conflict of interest

The authors declare that they have no conflict of interest.

References

AbdAlla S, Abdel-Baset A, Lother H, el Massiery A, Quitterer U (2005) Mesangial AT1/B2 receptor heterodimers contribute to angiotensin II hyperresponsiveness in experimental hypertension. *J Mol Neurosci* **26:** 185–192

AbdAlla S, Lother H, el Massiery A, Quitterer U (2001) Increased AT(1) receptor heterodimers in preeclampsia mediate enhanced angiotensin II responsiveness. *Nat Med* **7:** 1003–1009

Ahn S, Wei H, Garrison TR, Lefkowitz RJ (2004) Reciprocal regulation of angiotensin receptor-activated extracellular signal-regulated kinases by beta-arrestins 1 and 2. *J Biol Chem* **279:** 7807–7811

Angers S, Salahpour A, Joly E, Hilairet S, Chelsky D, Dennis M, Bouvier M (2000) Detection of beta 2-adrenergic receptor dimerization in living cells using bioluminescence resonance energy transfer (BRET). *Proc Natl Acad Sci USA* **97:** 3684–3689

Barki-Harrington L (2004) Oligomerisation of angiotensin receptors: novel aspects in disease and drug therapy. *J Renin Angiotensin Aldosterone Syst* **5:** 49–52

Bensaid M, Gary-Bobo M, Esclangon A, Maffrand JP, Le Fur G, Oury-Donat F, Soubrie P (2003) The cannabinoid CB1 receptor antagonist SR141716 increases Acrp30 mRNA expression in adipose tissue of obese fa/fa rats and in cultured adipocyte cells. *Mol Pharmacol* **63:** 908–914

Billet S, Aguilar F, Baudry C, Clauser E (2008) Role of angiotensin II AT1 receptor activation in cardiovascular diseases. *Kidney Int* **74:** 1379–1384

Billet S, Bardin S, Verp S, Baudrie V, Michaud A, Conchon S, Muffat-Joly M, Escoubet B, Souil E, Hamard G, Bernstein KE, Gasc JM, Elghozi JL, Corvol P, Clauser E (2007) Gain-of-function mutant of angiotensin II receptor, type 1A, causes hypertension and cardiovascular fibrosis in mice. *J Clin Invest* **117:** 1914–1925

Breit A, Gagnidze K, Devi LA, Lagace M, Bouvier M (2006) Simultaneous activation of the delta opioid receptor (deltaOR)/sensory neuron-specific receptor-4 (SNSR-4) hetero-oligomer by the mixed bivalent agonist bovine adrenal medulla peptide 22 activates SNSR-4 but inhibits deltaOR signaling. *Mol Pharmacol* **70:** 686–696

Carriba P, Ortiz O, Patkar K, Justinova Z, Stroik J, Themann A, Muller C, Woods AS, Hope BT, Ciruela F, Casado V, Canela EI, Lluis C, Goldberg SR, Moratalla R, Franco R, Ferre S (2007) Striatal adenosine A2A and cannabinoid CB1 receptors form functional heteromeric complexes that mediate the motor effects of cannabinoids. *Neuropsychopharmacology* **32:** 2249–2259

Carroll RC, Morielli AD, Peralta EG (1995) Coincidence detection at the level of phospholipase C activation mediated by the m4 muscarinic acetylcholine receptor. *Curr Biol* **5:** 536–544

 ©2011 European Molecular Biology Organization

Chun HJ, Ali ZA, Kojima Y, Kundu RK, Sheikh AY, Agrawal R, Zheng L, Leeper NJ, Pearl NE, Patterson AJ, Anderson JP, Tsao PS, Lenardo MJ, Ashley EA, Quertermous T (2008) Apelin signaling antagonizes Ang II effects in mouse models of atherosclerosis. *J Clin Invest* **118:** 3343–3354

Clauser E, Curnow KM, Davies E, Conchon S, Teutsch B, Vianello B, Monnot C, Corvol P (1996) Angiotensin II receptors: protein and gene structures, expression and potential pathological involvements. *Eur J Endocrinol* **134:** 403–411

Cubero FJ, Nieto N (2008) Ethanol and arachidonic acid synergize to activate Kupffer cells and modulate the fibrogenic response via tumor necrosis factor alpha, reduced glutathione, and transforming growth factor beta-dependent mechanisms. *Hepatology* **48:** 2027–2039

Davies E, Bonnardeaux A, Plouin PF, Corvol P, Clauser E (1997) Somatic mutations of the angiotensin II (AT1) receptor gene are not present in aldosterone-producing adenoma. *J Clin Endocrinol Metab* **82:** 611–615

Ellis J, Pediani JD, Canals M, Milasta S, Milligan G (2006) Orexin-1 receptor-cannabinoid CB1 receptor heterodimerization results in both ligand-dependent and -independent coordinated alterations of receptor localization and function. *J Biol Chem* **281:** 38812–38824

Friedman SL (2008) Hepatic stellate cells: protean, multifunctional, and enigmatic cells of the liver. *Physiol Rev* **88:** 125–172

Gomes I, Grushko JS, Golebiewska U, Hoogendoorn S, Gupta A, Heimann AS, Ferro ES, Scarlata S, Fricker LD, Devi LA (2009) Novel endogenous peptide agonists of cannabinoid receptors. *FASEB J* **23:** 3020–3029

Gonzalez-Maeso J, Ang RL, Yuen T, Chan P, Weisstaub NV, Lopez-Gimenez JF, Zhou M, Okawa Y, Callado LF, Milligan G, Gingrich JA, Filizola M, Meana JJ, Sealfon SC (2008) Identification of a serotonin/glutamate receptor complex implicated in psychosis. *Nature* **452:** 93–97

Gupta A, Decaillot FM, Gomes I, Tkalych O, Heimann AS, Ferro ES, Devi LA (2007) Conformation state-sensitive antibodies to G-protein-coupled receptors. *J Biol Chem* **282:** 5116–5124

Gupta A, Mulder J, Gomes I, Rozenfeld R, Bushlin I, Ong E, Lim M, Maillet E, Junek M, Cahill CM, Harkany T, Devi LA (2010) Increased abundance of opioid receptor heteromers after chronic morphine administration. *Sci Signal* **3:** ra54

Hilairet S, Bouaboula M, Carriere D, Le Fur G, Casellas P (2003) Hypersensitization of the Orexin 1 receptor by the CB1 receptor: evidence for cross-talk blocked by the specific CB1 antagonist, SR141716. *J Biol Chem* **278:** 23731–23737

Ito M, Oliverio MI, Mannon PJ, Best CF, Maeda N, Smithies O, Coffman TM (1995) Regulation of blood pressure by the type 1A angiotensin II receptor gene. *Proc Natl Acad Sci USA* **92:** 3521–3525

Jeong WI, Osei-Hyiaman D, Park O, Liu J, Batkai S, Mukhopadhyay P, Horiguchi N, Harvey-White J, Marsicano G, Lutz B, Gao B, Kunos G (2008) Paracrine activation of hepatic CB1 receptors by stellate cell-derived endocannabinoids mediates alcoholic fatty liver. *Cell Metab* **7:** 227–235

Kearn CS, Blake-Palmer K, Daniel E, Mackie K, Glass M (2005) Concurrent stimulation of cannabinoid CB1 and dopamine D2 receptors enhances heterodimer formation: a mechanism for receptor cross-talk? *Mol Pharmacol* **67:** 1697–1704

Kunos G, Osei-Hyiaman D, Batkai S, Sharkey KA, Makriyannis A (2009) Should peripheral CB(1) cannabinoid receptors be selectively targeted for therapeutic gain? *Trends Pharmacol Sci* **30:** 1–7

Kunos G, Osei-Hyiaman D, Liu J, Godlewski G, Batkai S (2008) Endocannabinoids and the control of energy homeostasis. *J Biol Chem* **283:** 33021–33025

Le TH, Kim HS, Allen AM, Spurney RF, Smithies O, Coffman TM (2003) Physiological impact of increased expression of the AT1 angiotensin receptor. *Hypertension* **42:** 507–514

Lieber CS, DeCarli LM (1989) Liquid diet technique of ethanol administration: 1989 update. *Alcohol Alcohol* **24:** 197–211

Ma'ayan A, Jenkins SL, Barash A, Iyengar R (2009) Neuro2A differentiation by Galphai/o pathway. *Sci Signal* **2:** cm1

Monnot C, Bihoreau C, Conchon S, Curnow KM, Corvol P, Clauser E (1996) Polar residues in the transmembrane domains of the type 1 angiotensin II receptor are required for binding and coupling. Reconstitution of the binding site by co-expression of two deficient mutants. *J Biol Chem* **271:** 1507–1513

Pereira RM, dos Santos RA, da Costa Dias FL, Teixeira MM, Simoes e Silva AC (2009) Renin-angiotensin system in the pathogenesis of liver fibrosis. *World J Gastroenterol* **15:** 2579–2586

Pignatari GC, Rozenfeld R, Ferro ES, Oliveira L, Paiva AC, Devi LA (2006) A role for transmembrane domains V and VI in ligand binding and maturation of the angiotensin II AT1 receptor. *Biol Chem* **387:** 269–276

Rives ML, Vol C, Fukazawa Y, Tinel N, Trinquet E, Ayoub MA, Shigemoto R, Pin JP, Prezeau L (2009) Crosstalk between GABAB and mGlu1a receptors reveals new insight into GPCR signal integration. *EMBO J* **28:** 2195–2208

Rozenfeld R, Devi LA (2007) Receptor heterodimerization leads to a switch in signaling: beta-arrestin2-mediated ERK activation by mu-delta opioid receptor heterodimers. *FASEB J* **21:** 2455–2465

Rozenfeld R, Devi LA (2008) Regulation of CB1 cannabinoid receptor trafficking by the adaptor protein AP-3. *FASEB J* **22:** 2311–2322

Rozenfeld R, Décaillot F, IJzerman AP, Devi LA (2006) Heterodimers of G protein-coupled receptors as novel and distinct drug targets. *Drug Discov Today Ther Strateg* **3:** 437–443

Sachse R, Shao XJ, Rico A, Finckh U, Rolfs A, Reincke M, Hensen J (1997) Absence of angiotensin II type 1 receptor gene mutations in human adrenal tumors. *Eur J Endocrinol* **137:** 262–266

Salata RA, Malhotra IJ, Hampson RK, Ayers DF, Tomich CS, Rottman FM (1992) Application of an immune-tolerizing procedure to generate monoclonal antibodies specific to an alternate protein isoform of bovine growth hormone. *Anal Biochem* **207:** 142–149

Schuppan D, Afdhal NH (2008) Liver cirrhosis. *Lancet* **371:** 838–851

Sleister HM, Rao AG (2001) Strategies to generate antibodies capable of distinguishing between proteins with $>90\%$ amino acid identity. *J Immunol Methods* **252:** 121–129

Sleister HM, Rao AG (2002) Subtractive immunization: a tool for the generation of discriminatory antibodies to proteins of similar sequence. *J Immunol Methods* **261:** 213–220

Sugaya T, Nishimatsu SI, Tanimoto K, Takimoto E, Yamagishi T, Imamura K, Goto S, Imaizumi K, Hisada Y, Otsuka A, Uchida H, Sugiura M, Fukuta K, Fukamizu A, Murakami K (1995) Angiotensin II type 1a receptor-deficient mice with hypotension and hyperreninemia. *J Biol Chem* **270:** 18719–18722

Teixeira-Clerc F, Julien B, Grenard P, Tran Van Nhieu J, Deveaux V, Li L, Serriere-Lanneau V, Ledent C, Mallat A, Lotersztajn S (2006) CB1 cannabinoid receptor antagonism: a new strategy for the treatment of liver fibrosis. *Nat Med* **12:** 671–676

Tiyerili V, Zimmer S, Jung S, Wassmann K, Naehle CP, Lutjohann D, Zimmer A, Nickenig G, Wassmann S (2010) CB1 receptor inhibition leads to decreased vascular AT1 receptor expression inhibition of oxidative stress improved endothelial function. *Basic Res Cardiol* **105:** 465–477

Turu G, Simon A, Gyombolai P, Szidonya L, Bagdy G, Lenkei Z, Hunyady L (2007) The role of diacylglycerol lipase in constitutive and angiotensin AT1 receptor-stimulated cannabinoid CB1 receptor activity. *J Biol Chem* **282:** 7753–7757

Urtasun R, Cubero FJ, Vera M, Nieto N (2009) Reactive nitrogen species switch on early extracellular matrix remodeling via induction of MMP1 and TNFalpha. *Gastroenterology* **136:** 1410–1422, e1411–1414

Wager-Miller J, Westenbroek R, Mackie K (2002) Dimerization of G protein-coupled receptors: CB1 cannabinoid receptors as an example. *Chem Phys Lipids* **121:** 83–89

©2011 European Molecular Biology Organization